Available online at www.sciencedirect.com
ScienceDirect
Bioorganic & Medicinal Chemistry Letters 17 (2007) 4001–4005
Bioorganic & Medicinal Chemistry Letters

Synthesis and preliminary evaluation of mono-[^{123}I]iodohypericin monocarboxylic acid as a necrosis avid imaging agent

Humphrey Fonge,[a] Lixin Jin,[a] Huaijun Wang,[b] Yicheng Ni,[b] Guy Bormans[a] and Alfons Verbruggen[a,*]

[a]*Laboratory of Radiopharmacy, Faculty of Pharmaceutical Sciences, K.U. Leuven, BE-3000 Leuven, Belgium*
[b]*Department of Radiology, Faculty of Medicine, K.U. Leuven, BE-3000 Leuven, Belgium*

Received 19 March 2007; revised 20 April 2007; accepted 25 April 2007
Available online 30 April 2007

Abstract—Hypericin monocarboxylic acid was synthesized in an overall yield of 25% in four steps and radiolabelled with iodine-123 in good yield (>75%). The resulting mono-[^{123}I]iodohypericin monocarboxylic acid was evaluated in normal mice and in rats with ethanol induced liver necrosis. In this model, tracer concentration in necrotic liver tissue was 14 times higher than in the viable liver tissue as quantified by autoradiography at 24 h post injection. The results indicate the feasibility of visualization of necrotic tissue with the novel tracer.

Cell death occurs by two distinct processes, that is, programmed cell death (apoptosis) and necrosis.[1,2] Apoptosis can be initiated by several physiological stimuli that trigger a preprogrammed cellular set of events involving the activation and release of caspases which in turn command a structured cell destruction and removal. Necrosis, on the other hand, is caused by mechanical, thermal, electrical or noxious chemical injury and by profound hypoxia, ischaemia or even respiratory poisons such as cyanide. Both forms of cell death have been implicated in some diseases, for example in acute myocardial infarction (AMI). ^{99m}Tc-pyrophosphate, ^{111}In-antimyosin Fab antibody and ^{99m}Tc-glucarate have all been used in nuclear medicine to locate and quantify infarct size but none has optimal imaging characteristics.[3,4]

Percutaneous ethanol injection (PEI) is widely used to kill small tumuors (especially hepatocellular carcinomas) but a radiopharmaceutical to monitor response to this therapy[5,6] has not yet been developed. Upon PEI, tumuor cells die by necrosis and a radiolabelled necrosis avid agent may enable quantification of the necrotic tumuor volume after PEI treatment as well as guide subsequent treatments.

Our group has been focusing on infarct avid agents for contrast enhancement in magnetic resonance imaging (MRI) and single photon emission computer tomography (SPECT).[7–9] We have shown that mono-[^{123}I]iodohypericin ([^{123}I]MIH), an iodine-123 labelled derivative of hypericin (Fig. 1A), is very avid for necrotic[9] but not apoptotic (results unpublished) tissue in different animal models of necrosis and apoptosis. Because of the slow plasma clearance of [^{123}I]MIH, early in vivo visualization (2 h post tracer injection) of necrotic tissue in experimentally reperfused acute myocardial infarction (AMI) was not possible using [^{123}I]MIH in combination with single photon emission computerized tomography (SPECT).[10] We hypothesized that a less lipophilic derivative of hypericin would have a faster clearance from circulation and therefore permit earlier

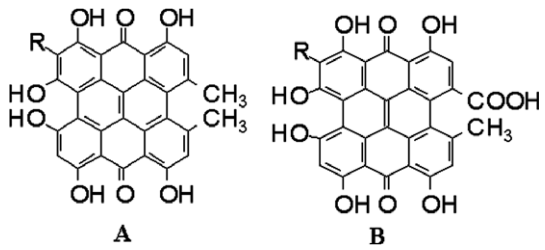

Figure 1. Structures of (A) R = H = hypericin and R = ^{123}I = mono-[^{123}I]iodohypericin and (B) R = H = hypericin monocarboxylic acid and R = ^{123}I = mono-[^{123}I]iodohypericin monocarboxylic acid.

Keywords: Mono-[^{123}I]iodohypericin monocarboxylic acid; Necrosis avidity; Autoradiography.
* Corresponding author. Tel.: +32 16330441; fax: +32 16330449; e-mail: alfons.verbruggen@pharm.kuleuven.be

0960-894X/$ - see front matter © 2007 Elsevier Ltd. All rights reserved.
doi:10.1016/j.bmcl.2007.04.083

visualization of necrotic tissue. This study reports the synthesis of mono-[^{123}I]iodohypericin monocarboxylic acid ([^{123}I]MIHA, Fig. 1B), and its preliminary evaluation in normal mice and in rats with ethanol induced liver necrosis. Avidity of [^{123}I]MIHA for necrotic liver was assessed ex vivo by gamma counting, autoradiography and triphenyltetrazolium (TTC), haematoxylin and eosin (H&E) staining techniques.

Protohypericin monocarboxylic acid (**4**) was obtained starting from emodin (**1**) by a modification of a reported four-step procedure[11] in an overall yield of 25% (Scheme 1a). Emodin was first acetylated to yield mainly tri-acetyl-emodin (**2**)[12] which upon oxidation yielded triacetyl-emodic acid (**3**).[13] Dimerization of **1** and **3** in the presence of hydroquinone as a free radical scavenger yielded protohypericin monocarboxylic acid (**4**)[14] which was readily converted to hypericin monocarboxylic acid (**5**) by photocyclization during irradiation of **4** with a 400-W halogen lamp for 30 min. ^{1}H NMR of **4** was recorded on a Gemini 200 MHz spectrometer and corresponded with previously reported δ-values.[11] Hypericin monocarboxylic acid (**5**) was used as precursor for the synthesis of the unlabelled mono-iodo-derivative (**6**) by a standard electrophilic substitution reaction employing iodide in the presence of peracetic acid as an in situ oxidizing agent.[15,16] The resulting compound was purified by HPLC and its identity was confirmed by mass spectrometry. Synthesis of radiolabelled mono-[^{123}I]iodohypericin monocarboxylic acid ([^{123}I]MIHA) was carried out by radioiodination of protohyperin monocarboxylic acid (**4**) followed by cyclization of the proto-derivative by irradiation of the reaction mixture for 30 min with a 400-W halogen lamp (Scheme 1b).[17] The cyclization reaction proceeded quantitatively as monitored by HPLC analysis. The overall radiolabelling yield was >75% relative to starting iodine-123 activity. The radiolabelled compound ([^{123}I]MIHA) was purified by reversed phase HPLC after which the solvents were evaporated by a gentle flush of nitrogen and the tracer agent was formulated in water/polyethylene glycol 400 (PEG 400) 80/20 V/V for animal studies. The unlabelled compound was used for identity confirmation of the radioiodinated compound [^{123}I]-**6** after co-injection with the radiolabelled derivative on HPLC (Fig. 2). ^{1}H NMR of unlabelled MIH showed that the iodination occurs ortho to the 'bay' phenol[15] (most acidic phenol, pK_a = 1.7). We therefore suppose that the position of iodine in [^{123}I]MIHA is as presented in Figure 1B.

The log octanol/buffer (0.025 M phosphate buffer, pH 7.4) partition coefficient (log P) of [^{123}I]MIHA was found to be 1.47 ± 0.06 (n = 6). The log P of [^{123}I]MIH is 3.08.[15] As expected the substitution of a carboxylic function for a methyl group has a profound effect on the lipophilicity of the compound.

Biodistribution of [^{123}I]MIHA was studied in normal NMRI mice after tail vein injection of 185 KBq. The mice were sacrificed by decapitation under anaesthesia at 30 min, 4 h or 24 h post injection (pi, n = 4 mice per time point). The organs were weighed and radioactivity was counted in a NaI(Tl) gamma counter and expressed as percentage of injected dose (ID)/organ and % ID/g of organ. Table 1 shows the biodistribution of [^{123}I]MIHA. Blood clearance of [^{123}I]MIHA (0.6% ID/g at 4 h pi) was much faster than for [^{123}I]MIH (28.2% ID/g at 4 h pi). Low blood clearance of [^{123}I]MIH has been attributed to its high affinity for plasma lipoproteins (data unpublished). The present data suggest that less the lipophilic [^{123}I]MIHA has much less affinity for plasma proteins resulting in enhanced plasma clearance. The tracer is mainly cleared via the hepatobiliary pathway resulting in high percentages excreted to the intestines and faeces. A significant amount of [^{123}I]MIHA was also cleared via the kidneys resulting in 21.1% ID of [^{123}I]MIHA in urine at 24 h pi compared to <6% ID of [^{123}I]MIH.

Preliminary evaluation of affinity of [^{123}I]MIHA for necrotic tissue has been performed in male adult Wistar rats (350–450 g) with hepatic necrosis. Hepatic necrosis was induced under laparotomy in seven rats by gradual infusion of 0.2 mL of ethanol into the left liver lobe. After closing the abdominal cavity with a two-layered suture, animals were allowed to recover for at least 12 h prior to tracer injection, during which the left liver lobe became necrotic. The rats were injected under anaesthesia via a tail vein with 22 MBq [^{123}I]MIHA and then sacrificed under anaesthesia by decapitation at 4 h (n = 4) or 24 h (n = 3) pi. The necrotic (left) and viable (right) liver lobes were harvested, rinsed with cold (4 °C) saline, weighed and counted in a gamma counter. Radioactivity concentration was expressed in counts per min (CPM) per gram tissue. The tissues were immediately stained in TTC (1.5% solution in saline) for 15 min at 37 °C and digitally photographed. They were then frozen to −80 °C and serial microtome sections (5–50 μm) were made from these frozen samples that were mounted on slides. Autoradiograms were made by exposing the slides to a high performance phosphor screen for 48 h. The screens were read with a phosphor imager and analysed using Optiquant® software. Afterwards the same slices were stained with H&E following the conventional procedure. Figure 3 shows representative ex vivo images after TTC staining (Fig. 3a) and autoradiography (Fig. 3b) of a 30-μm slice and the same slice after H&E staining (Fig. 3c) of the necrotic lobe (top row) and viable liver lobe (lower row) of a rat sacrificed at 24 h pi. Necrosis was confirmed by TTC staining (TTC negative areas) even though the images did not match with those of autoradiography and H&E staining due to disruptions that occurred during freezing and microtome sectioning. As can be seen from the images, there was a good match between the autoradiograms (high tracer uptake red spots) and H&E stained sections, thus confirming that uptake of [^{123}I]MIHA was concentrated in the necrotic sections of the liver. On H&E stained slices, pink areas (eosinophilic) correspond to severely necrotic tissue while purple areas (haematoxyphilic) correspond to viable tissue. The ratio of necrotic:viable was 1.8 and 14 at 4 h and 24 h pi, respectively, as quantified by autoradiography. The ratio of necrotic:viable was 1.2 and 1.9 at 4 h and 24 h, respectively, by gamma count-

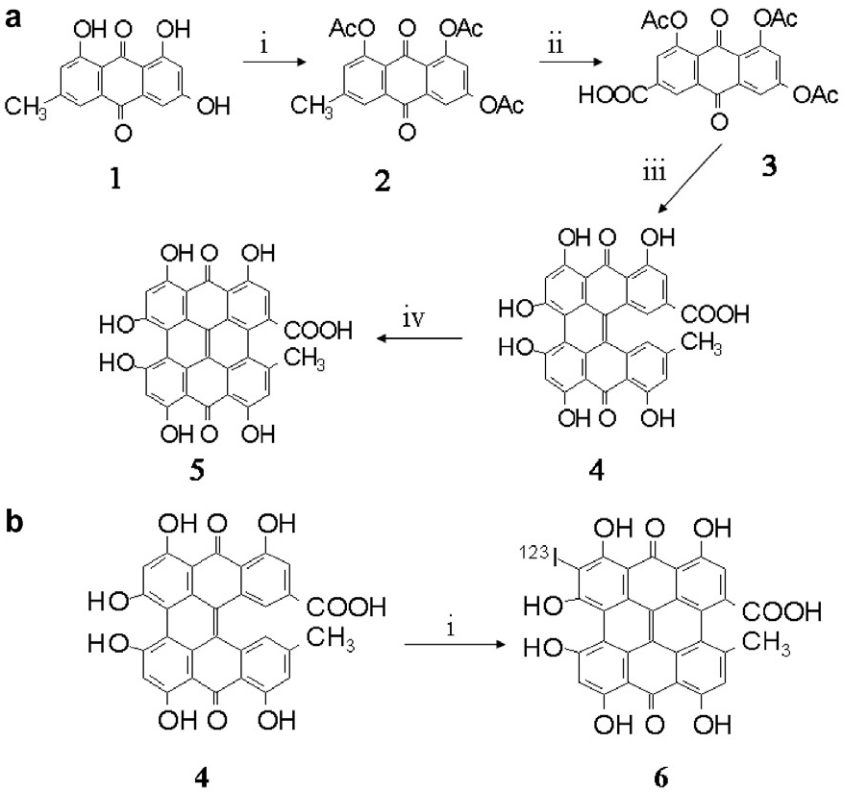

Scheme 1. Reagents and conditions: (a) (i) $(CH_3COO)_2$, 60 °C, 30 min; H_2SO_4; (ii) $CrO_3/CH_3COOH + (CH_3COO)_2$, 70 °C 3 h; (iii) **3 + 1** + C_6H_6O, 0.8 M KOH, 155 °C, 5 days; (iv) irradiation with 400-W halogen lamp for 30 min. (b) (i) [$^{123}I^+$], irradiation.

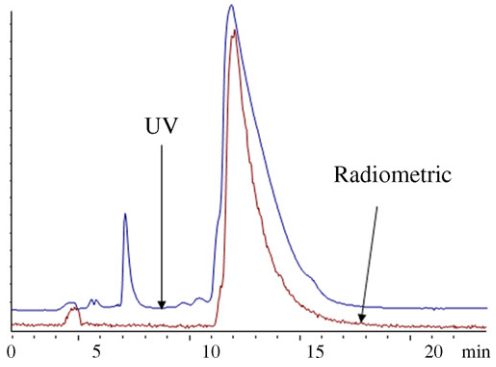

Figure 2. HPLC chromatogram after co-injection of unlabelled mono-iodohypericin monocarboxylic acid with mono-[^{123}I]iodohypericin monocarboxylic acid.

ing. The ratio was much less on gamma counting but this is due to the fact that viable cells are intermixed with necrotic cells, making sampling (separation of necrotic from viable tissue) very difficult.

In a liver model of reperfused hepatic infarction, the concentration of [^{123}I]MIH was 3.1 times higher in necrotic liver tissue compared to intact liver tissue as assessed by autoradiography at 24 h pi. [^{123}I]MIH has been shown to be very useful in delineation and sizing of infarcts in animal models of acute myocardial infarction (AMI).[10] In reperfused AMI, infarct: remote tissue ratios were as high as 81:1 and infarcts were well delineated at 9 h pi. Avidity of [^{123}I]MIHA for necrosis was higher than that of [^{123}I]MIH in a rat model with reper-

Table 1. Biodistribution of mono-[^{123}I]iodohypericin monocarboxylic acid ([^{123}I]MIHA) in normal NMRI mice

Organ	% injected dose (±SD)			% injected dose/g (±SD)		
	30 min	4 h	24 h	30 min	4 h	24 h
Bladder	0.3 (±0.1)	7.1 (±6.2)	21.1 (±9.8)	na	na	na
Kidneys	2.9 (±0.3)	2.6 (±0.2)	1.0 (±0.2)	4.4 (±0.4)	4.8 (±0.3)	1.9 (±0.4)
Liver	64.4 (±3.0)	22.4 (±5.8)	4.7 (±1.1)	33.7 (±2.5)	13.2 (±3.5)	2.7 (±0.9)
Spleen + pancreas	1.3 (±0.3)	0.5 (±0.2)	0.2 (±0.0)	3.9 (±0.4)	1.6 (±0.6)	0.5 (± 0.1)
Lungs	1.4 (±0.4)	0.3 (±0.1)	0.1 (±0.0)	5.0 (±1.7)	1.2 (±0.3)	0.2 (± 0.1)
Heart	0.5 (±0.1)	0.3 (±0.1)	0.1 (±0.0)	3.1 (±0.8)	1.9 (±0.6)	0.7 (±0.5)
Intestines + faeces	13.2 (±2.4)	50.5 (±12.5)	69.4 (±9.4)	na	na	na
Brain	0.0 (±0.0)	0.0 (±0.0)	0.0 (±0.0)	0.0 (±0.0)	0.0 (±0.0)	0.0 (±0.0)
Blood	3.3 (±1.5)	1.6 (±1.3)	0.1 (±0.0)	1.3 (±0.6)	0.6 (±0.5)	0.0 (±0.0)
Carcass	13.2 (±3.8)	10.3 (±6.6)	2.8 (±0.5)	na	na	na

SD, standard deviation; na, not applicable.

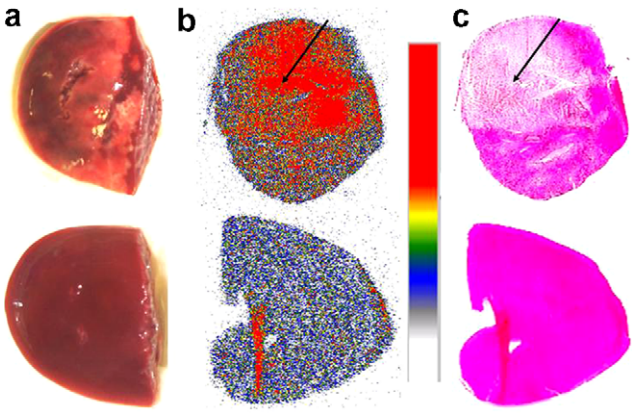

Figure 3. Ex vivo images of rat liver at 24 h post injection. (a) TTC stained liver lobes of necrotic (1st row) and viable (2nd row) liver tissue, (b) autoradiograms of 30-lm slice of necrotic (1st row) and viable (2nd row) tissue and (c) H&E stained slices of necrotic (1st row) and viable (2nd row) tissue. Arrows indicate regions of severe necrosis. Note perfect match between autoradiograms and H&E stained sections. Colour scale corresponds to autoradiograms.

fused hepatic infarction. Whether this difference was due to the different models used still has to be evaluated. In the occlusion–reperfusion model of liver infarction both apoptosis and necrosis can be induced with the extent of tracer uptake being influenced by the balance between both forms of cell death. Ethanol injection, on the other hand, specifically induces necrosis. Early delineation (2 h pi) of AMI using [^{123}I]MIH was not possible given the very high blood pool activity of the tracer agent at this time point (in mice there was namely 30.0, 28.2 and 0.7% ID/g at 30 min, 4 h and 24 h pi, respectively, assuming blood accounts to 7% of total body mass). In contrast, [^{123}I]MIHA showed a rapid blood clearance with 0.6% ID/g blood at 4 h pi. The rapid blood clearance of [^{123}I]MIHA could be an advantage over [^{123}I]MIH for imaging AMI as a good contrast could be obtained early enough to visualize AMI within the clinically relevant time window for thrombolysis (usually within 6 h of the acute event). This faster clearance from plasma and the major organs makes [^{123}I]MIHA an attractive and more favourable alternative for [^{123}I]MIH for imaging of AMI.

Several infarct avid imaging agents have been proposed and used in nuclear medicine, but none of them meets the optimal imaging characteristics. The most interesting has been ^{99m}Tc-glucarate which has been shown in several studies to be very useful in delineating and sizing myocardial infarcts in animals and in humans. ^{99m}Tc-glucarate imaging nonetheless presents with two limitations[18] which can be overcome by imaging using [^{123}I]MIH and [^{123}I]MIHA: (1) scan positivity with ^{99m}Tc-glucarate is limited to the early hours of the acute injury (typically < 9 h after AMI) and (2) it is rapidly washed out from the infarcted myocardium. [^{123}I]MIH as well as [^{123}I]MIHA have longer half lives in necrotic tissue, making it potentially feasible to image old as well as new infarcts.

This preliminary evaluation presents a good indication for the necrosis avidity of [^{123}I]MIHA. Further experiments will involve in vivo imaging to investigate the time during which the best target (necrosis) to non-target (viable tissue) ratios can be obtained. Single photon emission computer tomography (SPECT) imaging with [^{123}I]MIHA in this model of necrosis may find applications in the monitoring of response to PEI therapy. PEI therapy has been monitored until now by computer tomography (CT), which measures total tumuor volume rather than the percentage of cells killed by therapy, with a possibility of over- or underestimating the residual viable tumuor mass. Expanding infarct avid scintigraphy to PEI imaging would therefore be beneficial to both patients and clinicians. Imaging of AMI presents an even more challenging clinical task for which [^{123}I]MIHA will also be evaluated for its potential usefulness.

Acknowledgments

We appreciate the invaluable contribution of Peter Vermaelen in the animal experiments. This work was supported by a grant awarded by Geconcerteerde Onderzoeksactie (GOA) of the Flemish Government, FWO-Vlaanderen Grant G. 0257.05 and in part by the EC-FP6-project DiMI, LSHB-CT-2005-512146.

References and notes

1. Lennon, S. V.; Martin, S. J.; Cotter, T. G. *Cell Prolif.* **1991**, *24*, 203.
2. Darzynkiewicz, Z. *J. Cell Biochem.* **1995**, *58*, 151.
3. Jansen, D. E.; Corbett, J. R.; Wolfe, C. L.; Lewis, S. E.; Gabliani, G.; Filipchuk, N.; Redish, G.; Parkey, R. W.; Buja, L. M.; Jaffe, A. S.; Rude, R.; Sobel, B. E.; Willerson, J. T. *Circulation* **1985**, *72*, 327.
4. Khaw, B. A.; Yasuda, T.; Gold, H. K.; Leinbach, R. C.; Johns, J. A.; Kanke, M.; Barlai-Kovach, M.; Strauss, H. W.; Haber, E. *J. Nucl. Med.* **1987**, *28*, 1671.
5. Ferrari, F. S.; Stella, A.; Pasquinucci, P.; Vigni, F.; Civeli, L.; Pieraccini, M.; Magnolfi, F. *Eur. J. Gastroenterol. Hepatol.* **2006**, *18*, 659.
6. Shiina, S.; Teratani, T.; Obi, S.; Sato, S.; Tateishi, R.; Fujishima, T.; Ishikawa, T.; Koike, Y.; Yoshida, H.; Kawabe, T.; Omata, M. *Gastroenterology* **2005**, *129*, 122.
7. Ni, Y.; Cresens, E.; Adriaens, P.; Miao, Y.; Verbeke, K.; Dymarkowski, S.; Verbruggen, A.; Marchall, G. *Acad. Radiol.* **2002**, *9*, S98.
8. Ni, Y.; Bormans, G.; Chen, F.; Verbruggen, A.; Marchal, G. *Invest. Radiol.* **2005**, *40*, 526.
9. Ni, Y.; Huyghe, D.; Verbeke, K.; de Witte, P. A.; Nuyts, J.; Mortelmans, L.; Chen, F.; Marchal, G.; Verbruggen, A. M.; Bormans, G. M. *Eur. J. Nucl. Med. Mol. Imaging* **2006**, *33*, 595.
10. Fonge, H.; Vunckx, K.; Ni, Y.; Nuyts, J.; Mortelmans, L.; Wang, H.; de Groot, T.; Vermaelen, P.; Bormans, G.; Verbruggen, A. *Abstract of Papers*, 54th Annual Meeting of the Society of Nuclear Medicine, Washington, DC, The Society of Nuclear Medicine: Reston, VA, 2007; Abstract 610.
11. Gruszecka-Kowalik, E.; Zalkow, L. H. *Org. Prep. Proc. Int.* **2000**, *32*, 57.
12. To a mixture of 1 g (3.85 mmol) emodin (**1**) and 10 mL acetic anhydride was added dropwise 200 μL of 96% H_2SO_4under stirring. The reaction mixture was refluxed at

65 °C for 30 min. The resulting yellow solution was added to 50 mL of water and the yellow precipitate (**2**) so formed was washed with water and dried under reduced pressure. The precipitate **2** consisted of a mixture of di- and tri-acetylated emodin. Yield 99%. Accurate mass di-acetylated emodin $[C_{19}H_{14}O_7]^-$ theoretical 352.0739 Da, found 352.0694 Da.

13. 1.34 g (3.38 mmol) of **2** was dissolved in a mixture of 30 mL CH_3COOH and 30 mL acetic anhydride at 55–60 °C. A solution of 3 g CrO_3 in a mixture of 2.5 mL H_2O and 35 mL CH_3COOH was added dropwise over 30 min. The mixture was stirred at 70 °C for 3 h during which the brown solution turned green. It was then added to 1 L of water and the mixture was cooled overnight at 4 °C to precipitate the desired product (**3**) as a yellow powder. The powder was washed thoroughly with H_2O and dried over P_2O_5. Yield 98%. Accurate mass of tri-acetylated emodic acid $[C_{21}H_{14}O_{10}]^-$: theoretical 425.0514 Da, found 425.0547 Da.
14. 0.1 g of **1** (0.37 mmol), 0.32 g of **3** (0.75 mmol) and 0.162 g of hydroquinone (1.5 mmol) were dissolved in 5 mL of 0.8 M KOH protected from light in a capped vial placed in a heavy steel reaction vial holder. The vial was placed in an oven at 155 °C and allowed to react for 5 days during which it was agitated every 24 h to allow mixing. After cooling, the reaction mixture was acidified to pH 4–4.5 with 1 M HCl and the dark coloured precipitate was separated by centrifugation, after which the filtrate was extracted three times with 2% $NaHCO_3$ and EtOAc. The aqueous layer was evaporated in vacuo and the residue was dissolved in 25 mL methanol and applied on a silica gel column. Purification was afforded by gradient elution starting from 100% CH_2Cl_2 to CH_2Cl_2/MeOH (80:20 V/V). The first major fraction was collected, evaporated in vacuo and repurified on silica gel. Evaporation of solvents yielded the deep purple solid **4**. The residue was dissolved in dry methanol and the solution was irradiated with a 400-W halogen lamp for 30 min to give compound **5**. ^{1}H NMR **4** (DMSO) δ 7.96 (s, CH-11), 7.67 (s, CH-9), 7.28 (s, CH-14), 7.18 (s, CH-2, CH-5) 6.76 (s, CH-12), 2.50 (s, CH_3). Accurate mass of **5** $[C_{30}H_{14}O_{10}]^-$ theoretical 533.0510 Da, found 533.0478 Da, accurate mass of **4** $[C_{30}H_{16}O_{10}]^-$ theoretical 535.0703 Da, found 535.0671 Da.
15. Bormans, G.; Huyghe, D.; Christiaen, A.; Verbeke, K.; de Groot, T.; Vanbilloen, H.; de Witte, P.; Verbruggen, A. *J. Labelled Compd. Radiopharm.* **2004**, *47*, 191.
16. Unlabelled-**6**: To 15 mL of a 0.5 mg/mL solution of compound (**5**) in ethanol were successively added 2.5 mL of 0.5 M H_3PO_4, 5 mL of 0.2 M peracetic acid and 5 mL ethanol followed by dropwise addition of 1.1 mL of a 1 mg/mL solution of NaI in 0.01 M NaOH and stirring for a further 30 min. The volume of the solution was reduced in vacuo followed by purification of the residue using reversed phase HPLC (LaChrom Elite, Hitachi, Darmstadt, Germany) on a semi-preparative column (XTerra® prep RP_{18} 10 μm, 10 mm × 250 mm) using 0.05 M NH_4OAc/acetonitrile 60:40 V/V at a flow rate of 2.5 mL/min as mobile phase. Accurate mass $[C_{30}H_{13}IO_{10}]^-$: theoretical 658.9453 Da, found 658.9481 Da.
17. $[^{123}I]$-**6** was synthesized by successively adding 150 μL of a solution of 0.5 mg/mL of **4** in ethanol, 25 μL of 0.5 M H_3PO_4, 50 μL of 0.2 M peracetic acid and 50 μL ethanol to 37 MBq sodium[^{123}I]iodide (Amersham Biosciences, Diegem, Belgium) and incubating at room temperature for 30 min followed by photocyclization using a 400-W halogen lamp for 30 min. The resulting [^{123}I]MIHA was purified on reversed phase HPLC coupled with a radiometric detector (3-inch NaI(Tl) crystal) using an XTerra® C_{18} column (5 μm, 4.6 mm × 250 mm) with 0.05 M NH_4OAc/acetonitrile 60:40 V/V at a flow rate of 1 mL/min as mobile phase ($K' = 3.2$). [^{123}I]-6 was obtained in high specific activity (950 GBq/μmol).
18. Mariani, G.; Villa, G.; Rossettin, P. F.; Spallarossa, P.; Bezante, G. P.; Brunelli, C.; Pak, K. Y.; Khaw, B. A.; Strauss, H. W. *J. Nucl. Med.* **1999**, *40*, 1832.